

ChemComm

Accepted Manuscript



This is an *Accepted Manuscript*, which has been through the Royal Society of Chemistry peer review process and has been accepted for publication.

Accepted Manuscripts are published online shortly after acceptance, before technical editing, formatting and proof reading. Using this free service, authors can make their results available to the community, in citable form, before we publish the edited article. We will replace this *Accepted Manuscript* with the edited and formatted *Advance Article* as soon as it is available.

You can find more information about *Accepted Manuscripts* in the [Information for Authors](#).

Please note that technical editing may introduce minor changes to the text and/or graphics, which may alter content. The journal's standard [Terms & Conditions](#) and the [Ethical guidelines](#) still apply. In no event shall the Royal Society of Chemistry be held responsible for any errors or omissions in this *Accepted Manuscript* or any consequences arising from the use of any information it contains.

Productive encounter: Molecularly imprinted nanoparticles prepared using magnetic templates

Melanie Berghaus,¹ Reza Mohammadi^{1,3} and Börje Sellergren²

Received (in XXX, XXX) Xth XXXXXXXXX 20XX, Accepted Xth XXXXXXXXX 20XX DOI: 10.1039/b000000x

5 Synthesis of core shell nanoparticles by surface initiated reversible addition fragmentation chain transfer polymerization in presence of a chiral template conjugated to magnetic nanoparticles is reported. The approach leads to imprinted nanoparticles featuring enantioselectivity and enhanced affinity compared to nanoparticles prepared using free template.

Molecular imprinting is an established technique for producing polymers complementing specific molecules with respect to shape and functionality.¹⁻⁶ These molecularly imprinted polymers (MIPs) can now mimic antibodies with respect to both binding affinity and size and their ability to function in complex environments has considerably expanded the scope of applications e.g. receptor assays, sensors, affinity separations. The development of new and improved methods for producing these receptors is hence an urgent goal.

Most examples of high fidelity molecular imprinting have been demonstrated using highly cross-linked macroporous polymers as the imprinting matrix.⁴⁻⁶ In such amorphous polymers the templated sites are not uniform and hence binding curves do not follow a simple 1:1 ligand receptor binding model.⁷ Template occlusion is another recurring problem in traditional molecular imprinting. Typically a small fraction of the template added to the monomer mixture remains in the polymer matrix which can result in bleeding – a process detrimental in trace analysis.⁸ Moreover, template recovery and recycling is complicated and require multiple purification steps. Finally, traditional imprinting techniques are difficult to upscale, a fact seriously compromising commercial exploitation.

Several approaches addressing the aforementioned problems have been proposed. Thermodynamically controlled polymerizations^{9,10} or post-treatments such as thermal curing or annealing¹¹ are anticipated to reduce structural heterogeneity whereas the use of immobilized templates instead reduces binding site diversity, presumably due to a preferential orientation imposed by the interfacial confinement of the template.¹²⁻¹⁴ On the other hand, binding sites in imprinted nanoparticles experience less diverse microenvironments and, as for proteins, such particles can be affinity purified in order to further boost affinity.¹⁵⁻¹⁷ An elegant approach in this context is surface imprinting of nanoparticles by solid phase synthesis.¹⁸⁻²⁰

The nanoparticles are here synthesized in presence of template modified solid supports whereby growing particles adhere to the support surface. Post-synthesis, the particles can be affinity purified in situ leading to high affinity receptors in template free form. A limitation with the examples demonstrated thus far is related to the low specific surface area of the solid support beads. This translates into low particle yields (< 1 mg/g support beads) and a need for large reactors which essentially limits the technique to serial synthesis protocols.²¹

55 Here we introduce a novel scalable process to produce surface imprinted nanoparticles in high yield and in template free form. This is based on the use of nanosized magnetic placeholder templates (Figure 1) in a process tolerating high template concentrations. The increased product yield should make this method ideal for both small-scale parallel synthesis and large-scale synthesis by established polymerization techniques. In this report we demonstrate the feasibility of the concept focusing on an extensively studied model system combined with RAFT mediated polymerization²² from nanosized silica cores (Figure 65 S1).

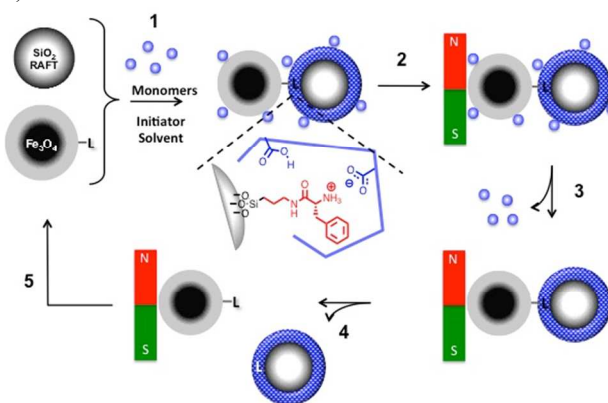


Figure 1. Principle of using magnetic templates for synthesis, affinity enrichment and purification of surface imprinted core shell micro and nanoparticles. (1) Polymerization of monomers in presence of the binary particle suspension, (2) Separating the magnetic template and polymers adhering to the template from the crude reaction mixture. (3) Washing off loosely bound unreacted monomers and oligomers, (4) Gradually releasing the polymer adhering to the magnetic template by physical or chemical means thereby enriching high affinity MIP particles. (5) Reuse of the magnetic template repeating steps 1-4.

Prior to introducing magnetic templates a procedure for producing core-shell imprinted nanoparticles using soluble template was developed. This relied on our previously reported procedure for surface initiated polymerization of methacrylic acid (MAA) and ethyleneglycol dimethacrylate (EGDMA) from mesoporous silica using L-phenylalanine anilide (L-PA) as template.^{10, 22}

The RAFT agent was coupled to the aminofunctionalized colloidal silica nanoparticles via the R-group according to Li et al.²³ resulting in surface coverages in accordance with our previous investigations for modification of mesoporous silicas (Table S1).^{10, 22} Each step was accompanied by probing the colloidal stability in different solvents. Hence, whereas the bare and aminofunctionalized colloidal core particles SiNP and SiNP-NH₂ formed stable dispersions in polar solvents (e.g. isopropanol, acetone, acetonitrile) the RAFT modified particles were partially aggregated nevertheless being well dispersible in alcohols such as isopropanol (Figure S2). The particles could be recovered by

either centrifugation at ca 3500rpm or by precipitation in hexane. Dynamic light scattering (DLS) resulting from the particles dispersed in isopropanol (SiNPs) or water (magNPs) showed Z-average particle sizes in rough agreement with particle and aggregate diameters estimated from corresponding TEM images (Figure S3) (Table 1).

Table 1. Z-average particle size and polydispersity from DLS of nanoparticles used in the study

Particle ^a	Diameter (nm)	Polydispersity
magNP	548	0.276
magNP@SiO ₂	605	0.206
magNP-NH ₂	442	0.101
magNP-L-Phe	281	0.216
SiNP	25	0.245
SiNP-NH ₂	32	0.183
SiNP-RAFT	65	0.341
SiNP-MIP2	45	0.255

a) The dispersing solvents were water (magNP) or isopropanol (SiNP).
 The specific surface areas by BET of magNP@SiO₂ and SiNP were 110 m²/g and 182 m²/g respectively.

Imprinted copolymers of MAA and EGDMA were then grafted from the supports according to Figure S1 and Table S2, i.e. in a 1:5 molar ratio of MAA to EGDMA in presence of ca 5 mol% of L-phenylalanine anilide (L-PA) as chiral template and with the beads dispersed in toluene. Grafting requires an external source of primary radicals which was here provided by a soluble initiator, added in substoichiometric amounts with respect to the RAFT agent.²² The quantity of monomer relative to the silica supports were adjusted to result in shells with approximately 4 nm thick shells. After polymerization the beads were isolated by centrifugation and subjected to repetitive washing-centrifugation cycles in order to remove any leachables (e.g. template, oligomers, unreacted monomers). Five cycles were sufficient for exhaustive template removal as concluded by HPLC analysis of the washing fractions. The beads were subsequently characterised by FTIR, TEM, DLS, TGA and elemental analysis. The FTIR spectra of the core shell beads shown in Figure S4 display two characteristic bands *i.e.* the carbonyl stretching of the polymer matrix at ca 1740 cm⁻¹ and the siloxane vibration of silica core at ca 1120 cm⁻¹. As expected, the ratio of these band intensities scale with the density of grafted polymer in agreement with corresponding data from mesoporous composites²² all in all indicating a successful grafting of the polymer shell.

In Table S2 the apparent thickness, calculated from the TGA mass loss data and elemental analysis, have been compared with the nominal thickness, estimated assuming the grafted shell to consist of monomers forming a liquid film covering the core surface. The somewhat lower measured thickness compared to the nominal values agrees with our previous report²² and can be attributed to solution chain growth, nevertheless resulting in an acceptable conversion of monomer to shell polymer. TEM images confirmed the core shell architecture with shells appearing brighter due to their lower electron density (Figure 2B). The images further revealed separate or smaller aggregates of polydisperse particles.

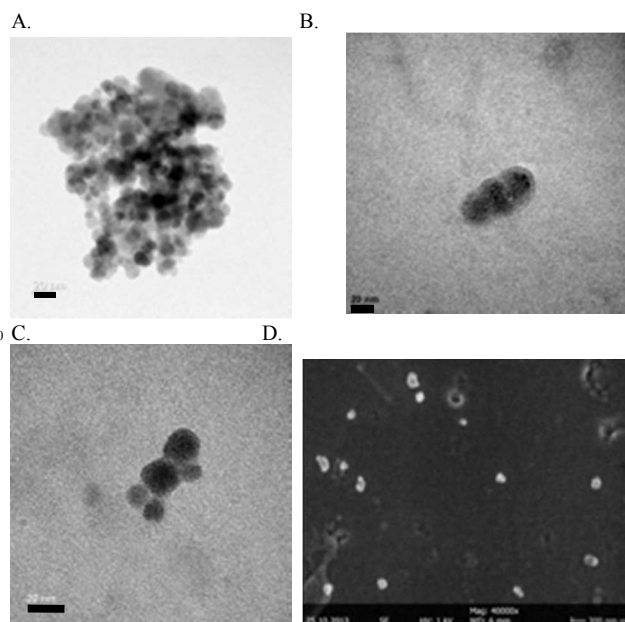


Figure 2. TEM (A-C) and SEM (D) images of magNP-L-Phe (A), the L-PA imprinted core shell nanoparticles SiNP-MIP1 (B) and SiNP-MIP2 (C and D). Scale bar = 20nm (A-C) or 300nm (D).

The particles were subsequently tested for their affinity towards the template L-PA and its optical antipode D-PA in acetonitrile. After incubating the particles with solutions of L-PA or D-PA of known concentrations the free concentration of the solutes were determined by reversed phase HPLC. Binding curves were then constructed (Figure 3) by plotting the specific amount of bound solute against the free concentration of solute.

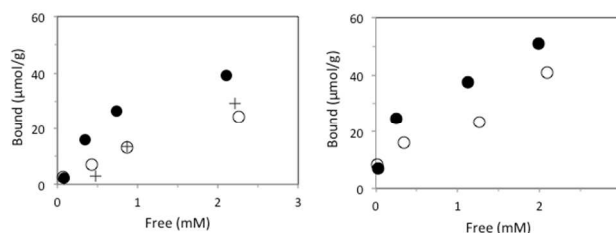


Figure 3. Binding curves of L-PA (solid symbols) and D-PA (open symbols) on imprinted (circles) and nonimprinted (crosses) core-shell particles in acetonitrile. A) L-PA imprinted SiNP-MIP1 and SiNP-NIP1, B) magNP-LPA imprinted SiNP-MIP2.

The curves display a distinct saturation behaviour with a clear preference for the templated L-form. In fact, the binding curve for the D-form coincides with the binding curve for the nonimprinted particles indicating the presence of highly discriminative imprinted sites. This also contrasts with binding curves reported for analogously prepared mesoporous materials where binding is weaker and less selective.²²

We then turned to the design of magnetic placeholder templates. Magnetite was chosen as a magnetic core, since this material can be obtained conveniently by the co-precipitation of Fe(II)/Fe(III) in aqueous media under base catalysis. A silica shell was then applied by aqueous hydrolysis of tetraethyl orthosilicate (TEOS) in MeOH and the resulting agglomerates (Figure 2A) characterised by DLS, FTIR and TEM. The TEM images (Figure

S6) revealed core particles in the desired size range of ~10 nm, visible crystal lattice planes (Figure S6 c,d) confirming the presence and precisely rendering the borders of magnetite cores and the presence of the silica shell.

The beads were then aminofunctionalized by reaction with APS followed by EDC catalyzed attachment of Fmoc-L-phenylalanine (Figure S1). Piperidine catalyzed deprotection yielded the template L-Phe attached via its carboxyl group to the aminofunctionalized surface as indicated by the appearance of the characteristic amide stretching bands (Figure S7) and by the release of fulvene-piperidine adduct upon Fmoc-Phe deprotection (Table S1). With the template modified magnetic beads at hand our next goal was to use them for affinity capture of the imprinted nanoparticles. Crucial in this context was the development of a colorimetric particle assay allowing facile quantification of soluble nonbound particles (Figure S8). This consisted of first converting the RAFT end groups to thiols through aminolysis followed by colorimetric detection of the thiol decorated colloidal particles by the established Ellman thiol assay.²⁴ Successful aminolysis was confirmed by disappearance of the pink color and the UV absorption band at 302 nm characteristic for the dithioester RAFT group (Figure S9). The aminolysed SiNP-MIP1 and SiNP-NIP1 were then incubated with magNP-L-Phe in acetonitrile followed by separation of the magnetic fraction. The magnetic fraction was subsequently washed three times with acetonitrile and three times with acidified methanol while collecting the particles with magnet between each washing step. The original incubation solution and each wash fraction were subsequently tested for nonbound particles using the Ellman assay. Figure 4 shows the normalized fraction of soluble particles remaining free after incubation with magNP-L-Phe.

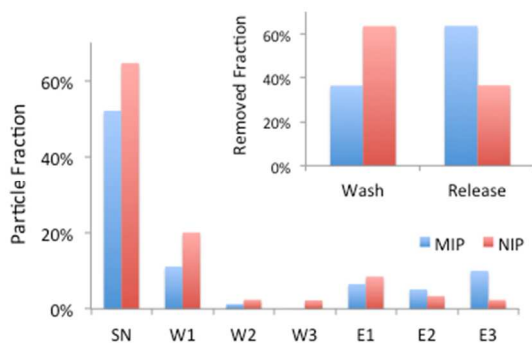


Figure 4. Distribution of nanoparticles SiNP-MIP1 (blue bars) and SiNP-NIP1 (red bars) (1mg/mL) in the fractions resulting from washing and elution of particles bound to magNP-L-Phe. SN=fraction of NPs remaining in supernatant after incubation and separation of the magnetic fraction, W1-W3=washes with 500 μ L acetonitrile, E1-E3=elution with MeOH/water/formic acid (80/5/15, v/v/v). The particle concentration was determined by the Ellman thiol assay and normalized with respect to particle concentration prior to fractionation.

It is clear from the relative abundance of free imprinted versus nonimprinted particles that the L-PA imprinted particles adhere more strongly to magNP-L-Phe, i.e. whereas ca 60% of the adhered imprinted particles are recovered in the elution fractions using the strongly acidified solutions only 40% was found when the nonimprinted particles were incubated. Hence, binding occurs in spite of the fact that L-Phe is coupled through an aliphatic linker resulting in a ligand only partially matching the structure of

the soluble template L-PA (featuring an aromatic amide substituent). This can be understood given the previously reported crossreactivities of L-PA versus L-phenylalanine ethyl amide imprinted polymers²⁵ and therefore the difference is not expected to compromise the affinity of the L-PA imprinted beads for magNP-L-Phe.

Conversely this would indicate that the magnetic ligand can serve as a template to generate binding sites complementary to L-PA. In order to test this hypothesis, the template modified magnetic particles were introduced to replace the soluble small molecular template in the previously described imprinting protocol. In this approach, polymerization occurs under homogenous conditions contrasting with the previously introduced approach for solid phase synthesis.^{18,26}

After magnetic collection, the magnetic fraction was washed followed by elution of the strongly bound particles by acidified methanol. Ca 17mg particles (SiNP-MIP2) were recovered in the elution fraction corresponding to an overall gravimetric yield of ca 9% assuming quantitative conversion of monomer to core shell polymer. Analysis of the different particle fractions by TGA (Figure S10) showed an increasing mass loss in the order magNP-L-Phe (4%), magNP-L-Phe/SiNP-MIP2 after washing (37%), magNP-L-Phe/SiNP-MIP2 prior to washing (40%) and released SiNP-MIP2 (43%). This order is expected assuming the aggregates to consist of silica core/polymer shell particles loosely and strongly adhered to magnetic FeO/SiO₂ particles. The purified SiNP-MIP2 were then characterised by FTIR, TEM, SEM and DLS. Collectively the data demonstrate the successful formation of nanoparticles (Figure 2C,D; Figure S11) with a Z-average size of 45 nm and a polydispersity of 0.255. The close agreement between the polydispersity index of SiNP-MIP2 and the silica core offers support for the anticipated core shell architecture. We next turned to the binding tests which were performed as for the particles prepared using the soluble template. Interestingly the material prepared using the magnetic placeholder template showed somewhat steeper binding curves and higher uptake of L-PA compared to SiNP-MIP1 (Figure 3B). Hence the immobilized ligand seems rather effective in generating imprinted sites complementary to L-PA. The enantioselectivity and affinity appears particularly striking given that the particles were generated using ca 10 times less template compared to the conventional procedure.

The here reported method profit from the high surface to volume ratio of template decorated magnetic nano-particles potentially allowing a much higher product yield of affinity enriched imprinted particles. In addition, the use of immobilized templates and RAFT mediated surface initiated polymerization should lead to more accessible and uniform binding sites. RAFT controlled precipitation polymerization is in this context known to create monodisperse nanoparticles with superior recognition properties.²⁷ These aspects in addition to the fact that polymerization take place in homogenous media hold great promise with respect to method scalability and parallel synthesis. We are currently exploiting these possibilities while applying the concept to other model systems including those of biological significance.

Notes and references

1) Faculty of Chemistry, Technical University of Dortmund, Otto-Hahn-Str.6, D-44221, Dortmund, Germany

2) Department of Biomedical Sciences, Faculty of Health and Society,

5 Malmö University, SE20506 Malmö, Sweden

Email: borje.sellergren@mah.se

3) Faculty of Chemistry, University of Tabriz, Tabriz, Iran

26. G. Pan, Y. Zhang, Y. Ma, C. Li and H. Zhang, *Angewandte Chemie Int. Ed.*, 2011, 50, 1-14.

1. X. Ding and P. A. Heiden, *Macromol. Mater. and Eng.*, 2014, 299, 268-282.
2. H. Zhang, *Polymer*, 2014, 55, 699-714.
3. R. Schirhagl, *Anal. Chem.*, 2014, 86, 250-261.
4. B. Sellergren and A. J. Hall, in *Supramolecular Chemistry: from Molecules to Nanomaterials*, eds. J. W. Steed and P. A. Gale, John Wiley & Sons Ltd, Chichester, UK, 2012, pp. 3255-3282.
5. L. Ye, (Ed.) *Molecular Imprinting: Principles and Applications of Micro- and Nanostructured Polymers*, Pan Stanford, 2013.
6. K. Haupt and C. Ayela (Eds.), *Molecular Imprinting*, Springer, 2012.
7. K. D. Shimizu, in *Molecularly Imprinted Materials: Science and Technology*, 2005, pp. 419-434.
8. A. Ellwanger, L. Karlsson, P. K. Owens, C. Berggren, C. Crencenzi, K. Ensing, S. Bayouhd, P. Cormack, D. Sherrington and B. Sellergren, *Analyst*, 2001, 126, 784-792.
9. A. D. Vaughan, S. P. Sizemore and M. E. Byrne, *Polymer*, 2007, 48, 74-81.
10. M. R. Halhalli, C. S. A. Aureliano, E. Schillinger, C. Sulitzky, M. M. Titirici and B. Sellergren, *Polymer Chemistry*, 2012.
11. Y. Chen, M. Kele, P. Sajonz, B. Sellergren and G. Guiochon, *Anal. Chem.*, 1999, 71, 928-938.
12. E. Yilmaz, K. Haupt and K. Mosbach, *Angew. Chem., Int. Ed.*, 2000, 39, 2115-2118.
13. a) M. M. Titirici, A. J. Hall and B. Sellergren, *Chemistry of Materials*, 2003, 15, 822-824. b) B. Sellergren, G. Büchel, WO 2001032760 A1 20010510 WO 2000-SE2083 20001026, SE 1999-3958 A 19991102, 1999
14. X. Shen X and L. Ye, *Macromolecules*, 2011, 44, 5631-5637.
15. Y. Hoshino, T. Kodama, Y. Okahata and K. J. Shea, *J. Am. Chem. Soc.* 2008, 130, 15242-15243.
16. A. R. Guerreiro, I. Chianella, E. Piletska, M. J. Whitcombe and S. A. Piletsky, *Biosensors and Bioelectronics*, 2009, 24, 2740-2743.
17. Y. Hoshino, W. W. Haberaecker, III, T. Kodama, Z. Zeng, Y. Okahata and K. J. Shea, *J. Am. Chem. Soc.*, 2010, 132, 13648-13650.
18. A. Poma, A. Guerreiro, M. J. Whitcombe, E. V. Piletska, A. P. F. Turner and S. A. Piletsky, *Adv. Funct. Mater.*, 2013, 23, 2821-2827.
19. I. Chianella, A. Guerreiro, E. Moczko, J. S. Caygill, E. V. Piletska, I. M. P. De Vargas Sansalvador, M. J. Whitcombe and S. A. Piletsky, *Anal. Chem.*, 2013, 85, 8462-8468.
20. S. Ambrosini, S. Beyazit, K. Haupt and B. Tse Sum Bui, *Chem. Commun.*, 2013, 49, 6746-6748.
21. A. Poma, A. Guerreiro, S. Caygill, E. Moczko and S. Piletsky, *RSC Advances*, 2014, 4, 4203-4206.
22. M. R. Halhalli, E. Schillinger, C. S. A. Aureliano and B. Sellergren, *Chem. Mater.*, 2012, 24, 2909-2919.
23. C. Li, J. Han, C. Y. Ryu and B. C. Benicewicz, *Macromolecules*, 2006, 39, 3175-3183.
24. G. Ellman, *Arch. Biochem. Biophys.* 1959, 82, 70-77
25. This can be understood given the previously reported crossreactivities of L-PA versus L-phenylalanine ethyl amide imprinted polymers (see B. Sellergren, M. Lepistö and K. Mosbach, *J. Am. Chem. Soc.*, 1988, 110, 5853-5860) and therefore the difference is not expected to compromise the affinity of the L-PA imprinted beads for magNP-L-Phe.
26. The outcome here depends on how the two types of nano-particles collide or aggregate as polymerization progresses. DLS of a solution of the reacting nano-particles dispersed in a polymerization mimicking solvent allowed some preliminary predictions in this regard. The results (Figure S12) revealed a tendency for SiNP-RAFT to associate to magNP-L-Phe. Such aggregates could be the precursor for imprinted particles which hence can be magnetically collected and enriched for particles exhibiting high affinity for the template.

